JPL Publication 97-5

Results of the 1996 JPL Balloon Flight Solar Cell Calibration Program

B. E. Anspaugh
R. S. Weiss

December 1, 1996

National Aeronautics and
Space Administration

Jet Propulsion Laboratory
California Institute of Technology
Pasadena, California

The research described in this publication was carried out by the Jet Propulsion Laboratory, California Institute of Technology, under a contract with the National Aeronautics and Space Administration.

ABSTRACT

The 1996 solar cell calibration balloon flight campaign was completed with the first flight on June 30, 1996 and a second flight on August 8, 1996. All objectives of the flight program were met. Sixty-four modules were carried to an altitude of 120,000 ft (36.6 km). Full I-V curves were measured on 22 of these modules, and output at a fixed load was measured on 42 modules. This data was corrected to 28°C and to 1 AU (1.496×10^8 km). The calibrated cells have been returned to the participants and can now be used as reference standards in simulator testing of cells and arrays.

ACKNOWLEDGMENT

The authors wish to express appreciation for the cooperation and support provided by the entire staff of the National Scientific Balloon Facility located in Palestine, Texas. Beverly St. Ange and Robert Mueller were very helpful in preparing the system for flight. The strong programmatic support from Art Chmielewski, Perry Bankston, Patricia Fournier, Patricia Zbylut and Julie Selders of JPL, and from Murray Hirschbein of NASA Headquarters is deeply appreciated. Special thanks is due this year to Roger Helizon and Carol Flores-Helizon who designed and built a Sun angle sensor for measuring the pointing accuracy of the solar tracker.

CONTENTS

Figures

Tables

"An expert is a person who may not have all the answers, but could get them if they would just give him a government grant."

Sagebrush Sven, Buffalo, Wyo.

1. INTRODUCTION AND OVERVIEW

The primary source of electrical power for unmanned space vehicles is the direct conversion of solar energy through the use of solar cells. As advancing cell technology continues to modify the spectral response of solar cells to utilize more of the Sun's spectrum, designers of solar cells and arrays must have the capability of measuring these cells in a light beam that is a close match to the solar spectrum. The solar spectrum has been matched very closely by laboratory solar simulators. But the design of solar cells and the sizing of solar arrays require such highly accurate measurements that the intensity of these simulators must be set very accurately. A small error in setting the simulator intensity can conceivably cause a disastrous missizing of a solar panel, causing either a premature shortfall in power or the launch of an oversized, overweight solar panel.

The Jet Propulsion Laboratory (JPL) solar cell calibration program was conceived to produce reference standards for the purpose of accurately setting solar simulator intensities. The concept was to fly solar cells on a high-altitude balloon, to measure their output at altitudes near 120,000 ft (36.6 km), to recover the cells, and to use them as reference standards. The procedure is simple. The reference cell is placed in the simulator beam, and the beam intensity is adjusted until the reference cell reads the same as it read on the balloon. As long as the reference cell has the same spectral response as the cells or panels to be measured, this is a very accurate method of setting the intensity. But as solar cell technology changes, the spectral response of the solar cells changes also, and reference standards using the new technology must be built and calibrated.

Until the summer of 1985, there had always been a question as to how much the atmosphere above the balloon modified the solar spectrum. If the modification was significant, the reference cells might not have the required accuracy. Solar cells made in recent years have increasingly higher blue responses, and if the atmosphere has any effect at all, it would be expected to modify the calibration of these newer blue cells much more than for cells made in the past.

In late 1984, a collection of solar cells representing a wide cross section of solar cell technology was flown on the shuttle Discovery as a part of the Solar Cell Calibration Facility (SCCF) experiment. The cells were calibrated as reference cells on this flight by using procedures similar to those used on the balloon flights. The same cells were then flown on the 1985 balloon flight and remeasured. Since the 2 sets of measurements gave nearly identical results (see reference 1), the reference standards from balloon flights may continue to be used with high confidence.

JPL has been flying calibration standards on high-altitude balloons since 1963 and continues to organize a calibration balloon flight at least once a year. Two balloon flights in 1996 were the 49th and 50th flights in this series. The 1996 flights incorporated 33 solar cell modules on the first flight and 31 on the second flight. There were a total of 8 different participants. The payload included Si, amorphous Si, GaAs, GaAs/Ge, dual junction cells, top and bottom sections of dual junction cells, and a triple junction cell.

A new data acquisition system was built for the balloon flights and flown for the first time on the 1995 flight. This system allows the measurement of current-voltage (I-V) curves for 19 modules, in addition to measurement of modules with fixed loads, as had been done in the past.

A Sun angle sensor was built and flown on the 1996 flights. This sensor measures the angle of the Sun in both azimuth and elevation and adds this information to the telemetry stream using four of the fixed-cell data channels.

2. PREFLIGHT PROCEDURES

2.1 MODULE FABRICATION

The cells were mounted by the participants or by JPL on JPL-supplied standard modules in accordance with standard procedures developed for the construction of reference cells. The JPL standard module is a machined copper or aluminum block on which a fiberglass circuit board is mounted. The circuit board has terminals that are used for making electrical connections to the solar cell and to a load resistor. On those cells slated for I-V measurement, no load resistor is connected. The circuit board can be modified to include 2 binding posts and a

jumper in series with one of the leads to the resistor. After flight calibration, the jumper can be removed and replaced with current pickoff probes for use on those pulsed xenon simulators that require a current input. The assembly is painted with either high-reflectance white or low-reflectance black paint. The resistor performs 2 tasks. First, it loads the cells near short-circuit current, which is the cell parameter that varies in direct proportion to light intensity. Second, it scales the cell outputs to read somewhat less than 100 mV during the flight, the maximum input voltage allowed by the data acquisition electronics for the fixed-load cells. Load resistance values are chosen to match the electrical characteristics of each cell flown. Nominally, the resistors will be $\approx$0.5 ohm for a 2 x 2 cm Si cell, 0.66 ohm for a 2 x 2 cm GaAs cell, 0.25 ohm for a 2 x 4 cm Si cell, etc. The load resistors are precision resistors (0.1%, 20 ppm/°C) and have a resistance stability equal to or better than $\pm$0.002% over a 3-year period. The solar cells are permanently glued to the body of the machined metal block with RTV 560 or its equivalent. This gives a good thermal conductivity path between the cells and the metal blocks, while providing electrical insulation between the rear surface of the solar cells and the block.

2.2 CELL MEASUREMENTS

After the cells were mounted on the blocks, the electrical output of each cell module was measured under illumination by the JPL X25 Mark II solar simulator. For these measurements, the simulator intensity was set by using only one reference cell—no attempt was made to match the spectral response of the reference standard to the individual cell modules. The absolute accuracy of these measurements is therefore unknown, but the measurements do allow checking of the modules for any unacceptable assembly losses or instabilities. After the balloon flight, the cells were measured in exactly the same way to check for any cell damage or instabilities that may have occurred as a result of the flight.

2.3 TEMPERATURE COEFFICIENTS AND LEAST SQUARES FITS

The temperature coefficients of the mounted cells were also measured before the flight. The modules were mounted in their flight configuration on a temperature-controlled block in a vacuum chamber. For the fixed-load cells, outputs were measured at 25, 35, 45, 55, 65, and 75°C under illumination with the X25 simulator. The temperature coefficients of the cell modules were computed by fitting the output vs temperature relationship with a linear least squares fit. The I-V cells were measured in open air at the same temperature schedule using the JPL Large Area Pulsed Solar Simulator (LAPSS) as the illumination source. Temperature coefficients for both short circuit current (I_{sc}) and open circuit voltage (V_{oc}) were computed using a linear least squares fit.

2.4 DATA ACQUISITION SYSTEM CHECKOUT AND CALIBRATION

The 1995 data acquisition (DAQ) system was used for the calibration measurements on the 1996 flights. This system is based on a 286 microprocessor in a ROM-DOS operating system. The program that controls the system is easily changed to match the requirements of each individual flight. This system also duplicates the function of the older data encoder with regard to reading and processing the outputs of the modules with fixed-load resistors (maximum input voltage of 100 mV). The system has 6 dedicated temperature measurement channels, now using platinum resistance sensors instead of thermistors. The system has the capability of measuring the I-V characteristics of as many as 19 solar cells and one reference channel. Loading of the cells to produce the I-V curves is accomplished by applying 20 resistive loads, one at a time, to each cell and measuring the cell's output voltage and current as each load is applied. Each cell has its own individually tailored set of 20 load resistors. The resistive loads are chosen to generate the expected I-V characteristic of each cell and to produce a large number of points near the maximum power (P_{max}) point. Sixteen resistors are available for cell loading. Selection of these resistors in parallel combinations of up to 5 at a time results in a theoretical total of 6,884 possible resistive loads, neglecting duplicates, available for each cell. A four-wire system is used for the I-V measurements, so that the wires measuring cell voltage do not carry cell current.

The heart of the DAQ is a 286-class computer on a STD bus circuit board. This computer controls the multiplexing of the cells, temperatures, calibration voltages, and power supply voltages for measurement. The computer is also used to connect each I-V cell in its turn to the measurement circuitry, and the computer also applies the specific set of load resistors across the cell under measurement. The computer is used to format the data, to add clock time, synch words, and a checksum for each line, and then to send all of this to the telemetry transmitter via an RS232 output. All of the test and measurement parameters are read out and transmitted during the course of a telemetry frame. During this time the fixed-load cells are each read 5 times, and each of the I-V cells are read once. All other engineering voltages and temperatures are also read once each frame. As

presently programmed, a telemetry frame is sent every 9.5 seconds.

All measurements of electrical parameters are performed by sending the signals through suitable amplifiers, and then to a 12-bit A/D converter. The fixed-load cell signals are sent through an amplifier with a gain of 49.775. The I-V cell voltage levels are sent through an amplifier with a gain of 2.000. Cell currents were passed through a precision 0.1-ohm resistor. The voltage drop across this resistor was fed to a differential amplifier with a gain of 52.62. The on-Sun indicator and the 7 temperature signals were each sent through individual amplifiers. All amplifiers went through an extensive calibration procedure prior to leaving JPL. Calibration voltages were available in the DAQ that could be used for monitoring the amplifiers used for voltage measurement during the flight. The Sun-angle-sensor data was sent through 4 of the fixed-load channels and incorporated into the telemetry stream.

The system is designed so that the output from the DAQ on the RS232 line can be fed directly to the COM input of a PC for preflight testing. During the flight, the RS232 output goes to the telemetry transmitter on the balloon, which transmits it to the telemetry receiver on the ground, which sends it to the COM input of the PC. This configuration allows a much more thorough checkout of the system before it leaves JPL.

The PC program for receiving, converting, and storing data is written in LabVIEW, a graphical programming language specifically designed for making engineering-type measurements under PC control. The LabVIEW program provides for graphical display of all the fixed-load cells simultaneously. The I-V curves of any or all of the 19 I-V cells may also be displayed. The program provides for digital readout of all power supply voltages, calibration voltages, temperatures, and on-Sun indicator readings. The Sun-angle-sensor data is displayed in the form of a scatter plot on the LabVIEW display. Synch status and checksum status are continuously displayed. These displays are continuously updated in real time and give an instantaneous reading on the status of the whole system.

2.5 PANEL ASSEMBLY AND CHECKOUT

After the electrical measurements of the solar cells were completed, the modules were mounted on the solar panel and connected electrically. Figures 1 and 2 are photographs of the mounted modules for the first and second flights, respectively. Figures 3 and 4 are corresponding diagrams that identify the modules by their serial numbers. After completion of the panel assembly, the panel, tracker, and DAQ were all given complete functional tests in terrestrial sunlight. The assembled tracker and panel were placed in sunlight on a clear, bright day and checked for the tracker's ability to acquire and track the Sun while each cell module was checked for electrical output. All power supply voltages and temperature readings were checked, and the calibration voltages were checked for stability and proper function. After these tests were completed satisfactorily, the assembly was shipped to the National Scientific Balloon Facility (NSBF) in Palestine, Texas for flight.

2.6 PRELAUNCH PROCEDURES AT PALESTINE

The NSBF was established in 1963 at Palestine, Texas. This location was chosen because it has favorable weather conditions for balloon launching and a large number of clear days with light surface winds. The high-altitude winds in this part of the country take the balloons over sparsely populated areas, so the descending payloads are unlikely to cause damage to persons or property. The JPL calibration flights have flown from the Palestine facility since 1973. The flights are usually scheduled to fly in the June-to-September time period, since the Sun is high in the sky at that time of year and the sunlight passes through a minimum depth of atmosphere before reaching the solar modules.

Upon arrival at Palestine, the tracker and module payload were again checked for proper operation. This included a checkout in an environmental test chamber wherein the tracker, calibration voltages, and the entire data acquisition system were all tested as a system. The chamber was pumped down to a pressure of $\approx$40 mb (0.4 N/cm^2)[corresponding to an altitude of 65,000 ft (19.8 km)], and the DAQ was cooled to -30°C. The system was tested at 10° increments during the cooldown. The assembly was then warmed up to +60°C, with tests occurring at each 10° increment. Then the assembly was removed from the environmental chamber and a room-temperature, end-to-end check was performed on the payload, telemetry, receiving, and decoding systems.

After all the checkouts and calibrations were performed, the tracker was mounted on an aluminum tubular hoop structure. This assembly was then mounted on the top portion (or apex) of the balloon. Figure 5 is a photograph of the tracker mounted on the hoop assembly. The solar panel is shown as it was configured for the second 1996 flight.

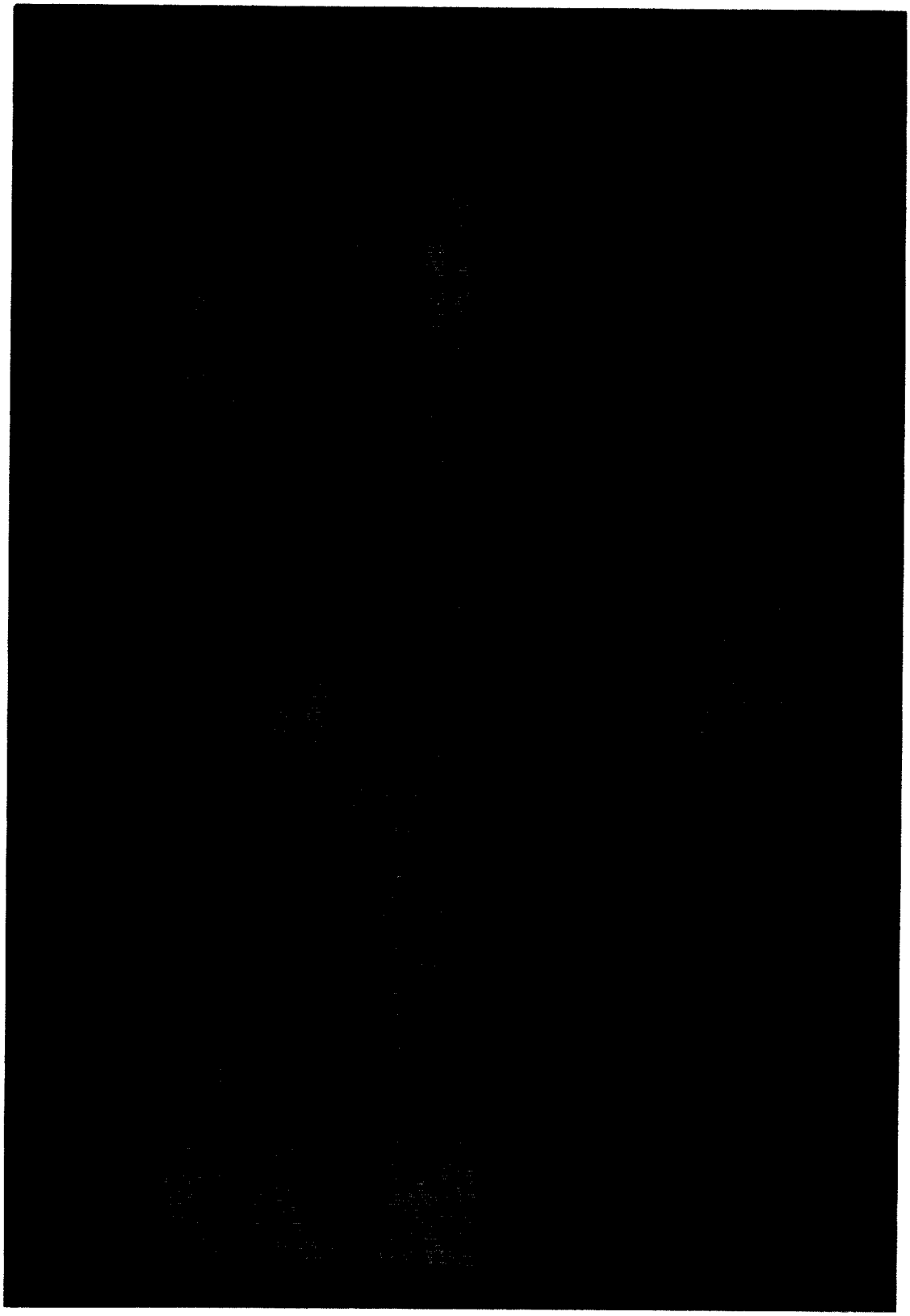

Figure 1. Photograph of the 1996-1 Balloon Flight Solar Panel

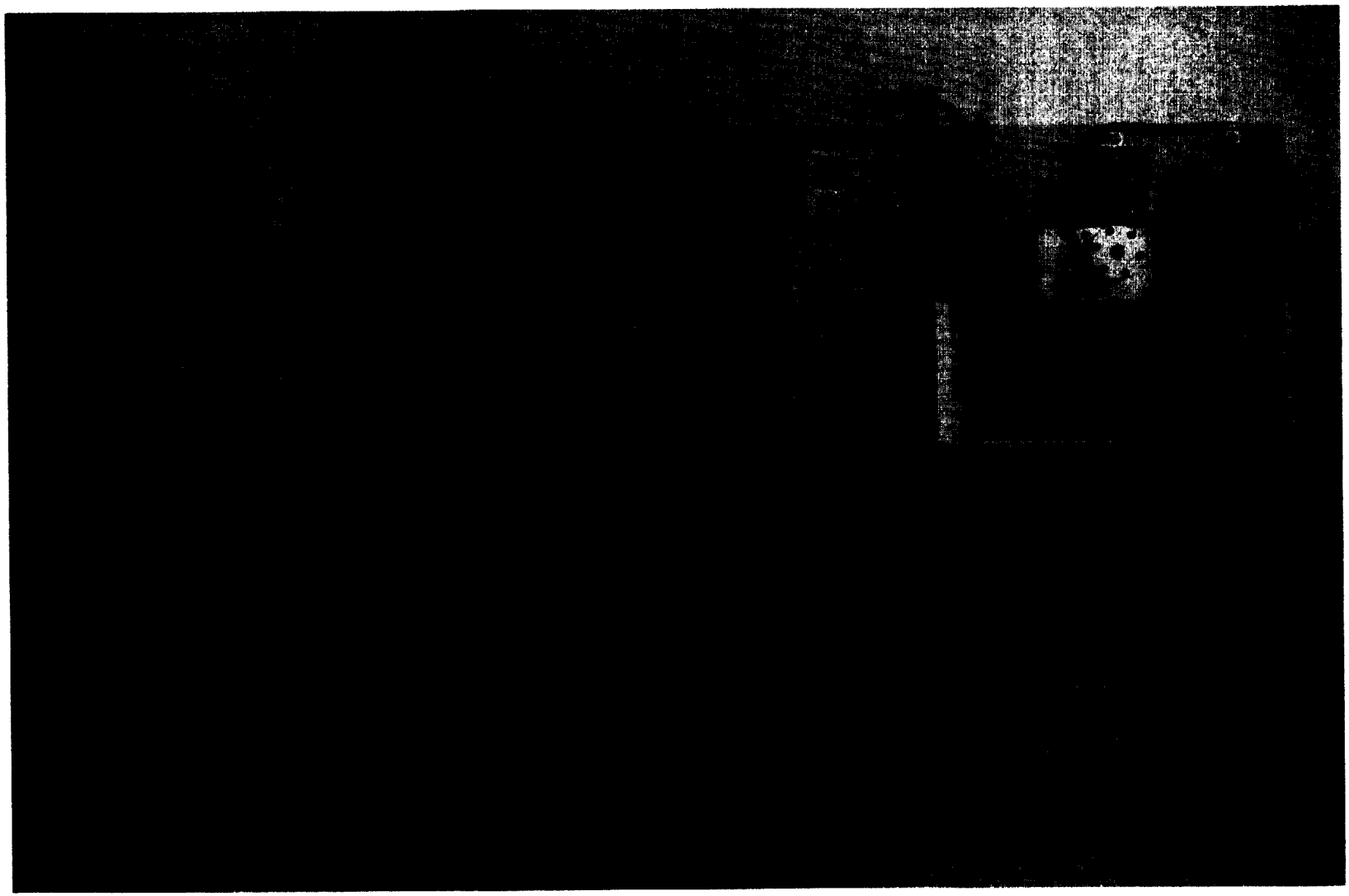

Figure 2. Photograph of the 1996-2 Balloon Flight Solar Panel

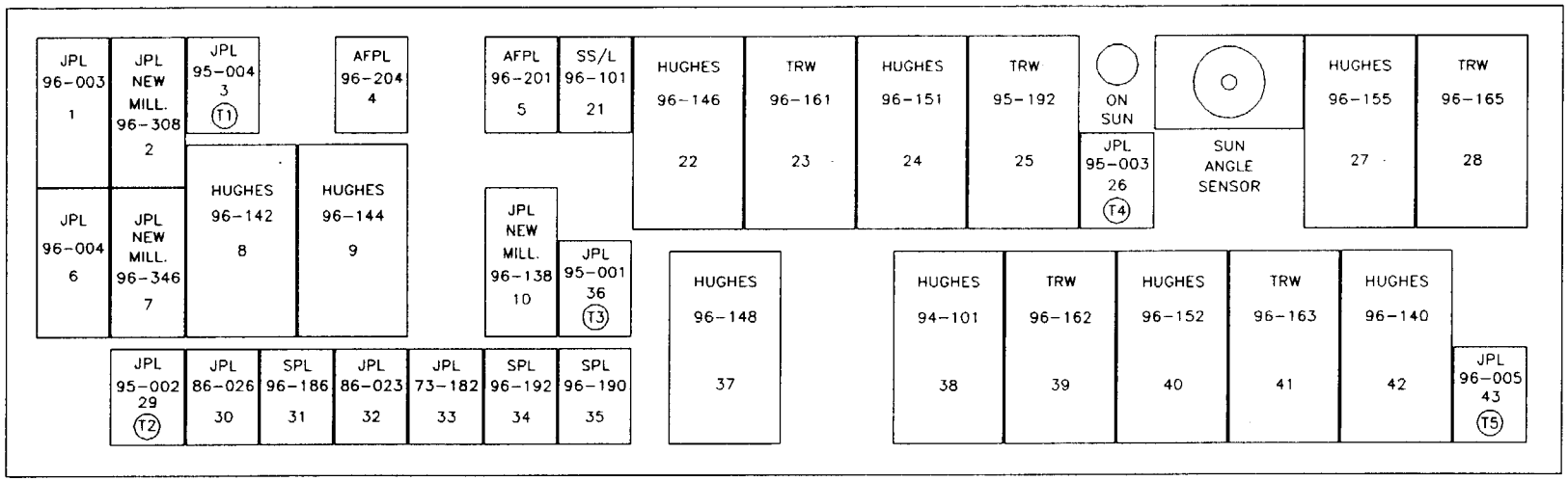

Figure 3. 1996-1 Module Location Chart

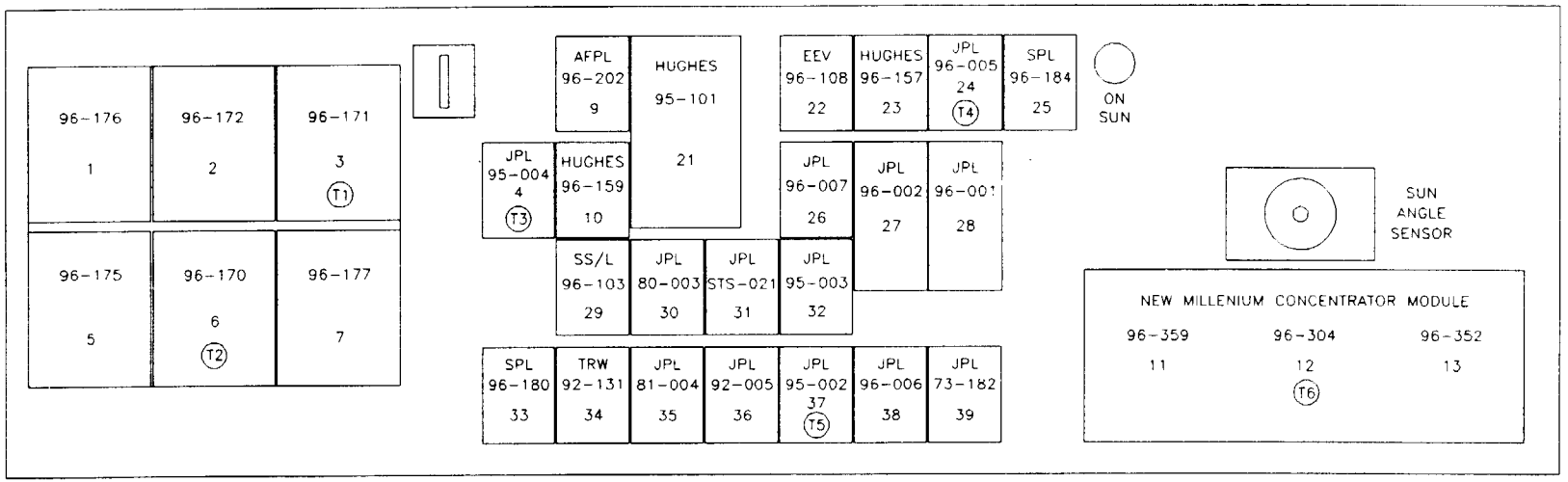

Figure 4. 1996-2 Module Location Chart

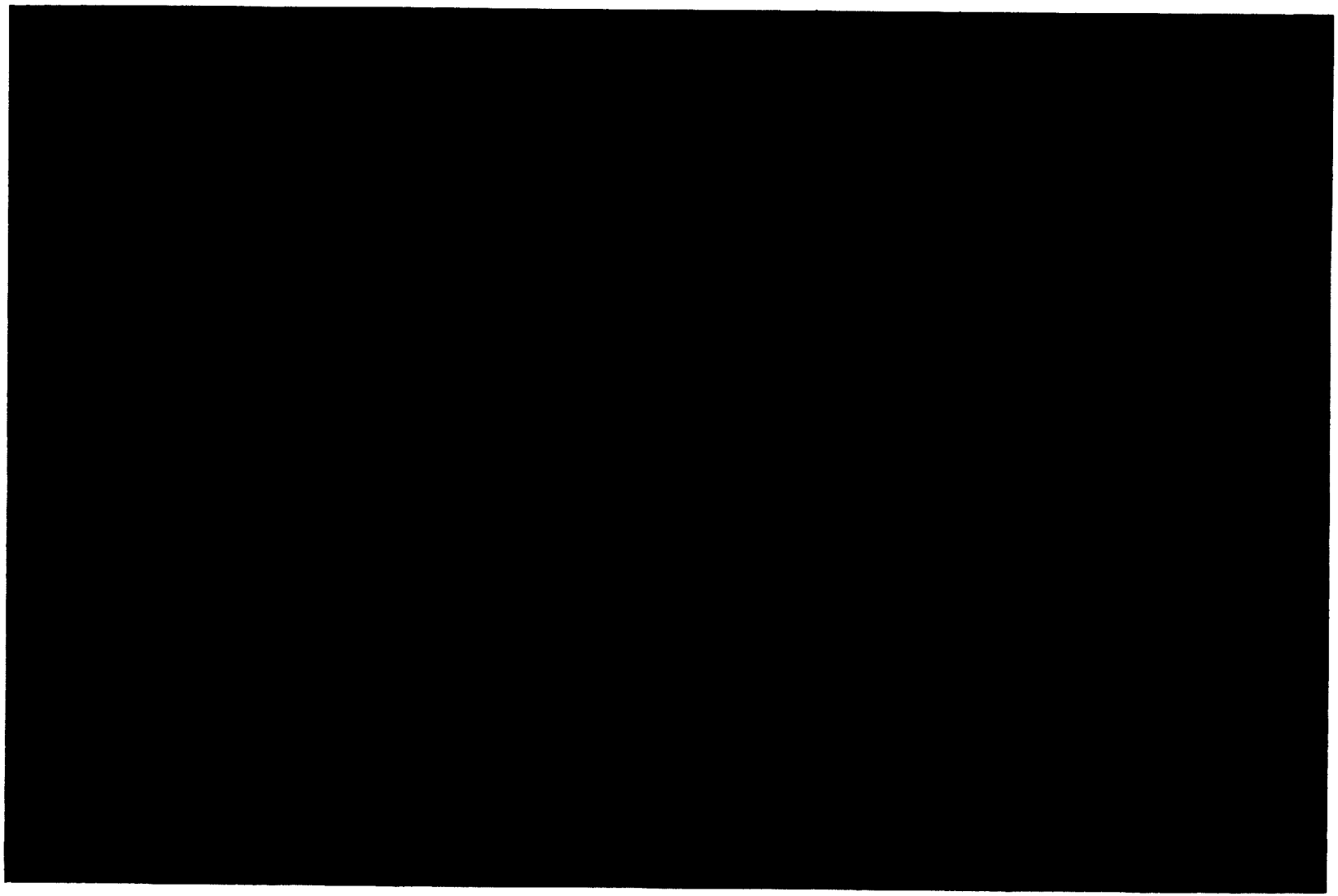

Figure 5. Tracker Mounted on Aluminum Hoop Assembly

3. BALLOON SYSTEM

The main components of the balloon flight system were (1) the apex-mounted hoop assembly that contained the experimental package, the data encoder, the recovery system, and the camera package; (2) the balloon; and (3) the lower payload that contained the telemetry and power systems.

3.1 BALLOON DESCRIPTION

The balloons used for the JPL solar cell calibration high-altitude flights have a volume of 3.46 million ft^3 (98,000 m^3). The balloon manufacturer used 0.8 mil (20 μm) polyethylene film (Stratofilm-372) designed specifically for balloon use. The balloon alone weighed 702 lb (319 kg). It was designed to lift itself and a payload weight of up to 725 lb (330 kg), distributed between the bottom and top payloads, to a float altitude of 120,000 ft (36.6 km). At float altitude, the balloon had a diameter of roughly 213 ft (65 m) and a height of 146 ft (45 m). To electrically connect the top and bottom payloads, a multiconductor cable was built into the balloon during its manufacture. The balloon was built with an internal rip line designed to rip a hole in the side of the balloon for termination of the flight. A special structure was built into the top of the balloon for attaching the top payload. Two poppet valves incorporated into this mounting structure can be commanded to open and release helium from the balloon at the end of the flight. The poppet valves act as a backup to the rip line.

Trying to inflate and launch a balloon with a sizable weight attached to its top is like trying to balance a cobra on top of a mongoose. A tow balloon tied to the top payload was used during the inflation and launch phases to add stability and to keep it on top. This smaller balloon, about 2,900 ft^3 (82 m^3), is designed to lift about 180 lb (82 kg). The tow balloon was cut loose from the top payload after the launch as soon as the main balloon stabilized and the launch-induced oscillations damped out.

3.2 TOP PAYLOAD

The top payload consisted of the tracker, solar panel, voltage reference box, multiplexer, DAQ, single-frame movie camera, clock, descent parachute, battery power supply for the tracker and data encoder, relay box, and tracking beacon. All these items were mounted to the aluminum hoop assembly as shown in Figure 5. The hoop assembly served the following functions:

(1) Permitted the top-mounted payload to "float" on top of the balloon and minimized billowing of balloon material around the top payload.

(2) Served as the mounting surface that attaches the top payload assembly to the balloon.

(3) Provided a convenient point for attaching the tow balloon and the descent parachute.

(4) Acted as a shock damper to protect and minimize damage to the top payload at touchdown.

The complete apex-mounted hoop assembly, as flown, weighed $\approx$130 lb (59 kg) and descended as a unit by parachute at flight termination.

The Sun tracker, shown in Figure 5, is capable of orienting the solar panel toward the Sun, compensating for the motion of the balloon by using two-axis tracking in both azimuth and elevation. The tracker has the capability to maintain its lock on the Sun to within $\pm$1 deg. To verify that the tracker was operating properly, the output of an on-Sun indicator was constantly monitored during the flight by feeding its output to the DAQ and entering its signal into the telemetry stream. The on-Sun indicator consists of a small, circular solar cell mounted at the bottom of a collimator tube, 7 in. (17.8 cm) long, with an aperture measuring 0.315 in. (0.8 cm) in diameter. The on-Sun indicator was attached to the solar panel so that it pointed at the Sun when the panel was perpendicular to the Sun. The output of the on-Sun indicator falls off very rapidly as the collimator tube points away from the Sun and provides a very sensitive indication of proper tracker operation. A Sun-angle-sensor was added to the system for the 1996 flights and gave a quantitative readout of the tracker's pointing accuracy.

A reflection shield was attached to the panel to prevent any stray reflected light from reaching any of the modules. This shield was made of sheet aluminum, painted black, and attached to three edges of the solar panel.

The solar cell modules were mounted onto the Sun tracker platform with an interface of Apiezon H vacuum grease and held in place with 4 screws. The grease was used to achieve a highly conductive thermal contact between the modules and the panel and to smooth out the temperature distribution over the solar panel as much as possible.

The solar panel temperature was monitored using platinum resistance sensors (RTDs). Some of the solar cell modules were constructed with RTDs embedded in the metal substrate directly beneath the solar cell. Six of these modules were mounted on the solar panel at strategic locations so that their temperature readings gave an accurate representation of panel temperature. Placement of these modules on the panel is shown in Figures 3 and 4. A seventh RTD was mounted inside the DAQ to monitor its temperature during environmental testing and during the flight.

An ultrawide-angle, single-frame movie camera mounted at the perimeter of the aluminum hoop provided visual documentation of tracker operation. A battery-powered timer activated the shutter at 10-second intervals, which meant that 50 ft (15.24 m) of super 8 movie film was sufficient to record the entire flight from launch to landing. A wind-up clock was placed in the camera's field of view for correlation of tracker operation with the telemetered data. The pictures provide a complete record of ascent, tracker operation at float altitude, descent, touchdown, and post-touchdown events.

A tracking or locator beacon was attached to the hoop assembly. This beacon, similar to those used for tracking wild animals in their natural habitat, consists of a low-wattage transmitter that sends short, 160-MHz pulses at the rate of about 1 per second. A hand-held directional antenna and a battery-powered receiver are used inside the chase plane and on the ground for locating the transmitter. This beacon has been very useful in locating this very small payload in a very large open range.

3.3 BOTTOM PAYLOAD

The bottom payload was entirely furnished by the NSBF. It consisted of a battery power supply, a ballast module for balloon control, a terminate package, and an electronics module known as the consolidated instrument package (CIP).

Power for operating most of the electrical and electronic equipment on the balloon was supplied by a high-capacity complement of lithium batteries. This supply, furnishing 28 Vdc regulated power and 36 Vdc unregulated power, powered all the instruments in the CIP. Several other small battery sources were used at various locations on the balloon for instruments that require small amounts of power. For example, the tracker and data encoder, the tracking beacons, the voltage reference box, and the camera timer all had individual battery power supplies. All batteries were sized to supply power for at least twice the expected duration of a normal flight.

High-altitude balloons tend to lose helium slowly during the course of the flight. As a consequence, a helium balloon will tend to reach float altitude and then begin a slow descent. To counteract this tendency, a ballast system was included as part of the bottom payload. It contained $\approx$100 lb (45 kg) of ballast in the form of very fine steel shot. The shot may be released in any desired amount by radio command. By proper use of this system, float altitude may be maintained to within $\pm$2,000 ft ($\pm$600 m).

The telemetry system was contained in the CIP. The system sent all data transmissions concerning the flight over a common RF carrier. The CIP also contained a command system for sending commands to the balloon for controlling scientific payloads or for controlling the housekeeping functions on the balloon. Specifically, the CIP contained the following equipment:

(1) Pressure transducers
(2) Subcarrier oscillators, as required
(3) An L-band FM transmitter
(4) .A Transponder for air traffic control tracking
(5) A Pulse Code Modulation (PCM) command receiver-decoder
(6) 2 Global Positioning Satellite (GPS) receivers

The altitude of the balloon was measured with a capacitance-type electronic transducer, manufactured by MKS Instruments, Inc., which read pressure within the range of 1,020 to 0.4 mbar (102,000 to 40 N/m^2) with an accuracy of 0.05%. The transducer produced a dc level that was encoded as PCM data and decoded at the receiving station into pressure, and the altitude was then calculated from the pressure reading. The GPS receivers also computed and sent altitude information into the telemetry stream.

The GPS navigation system was used for flight tracking. The second GPS receiver was used as a backup.. An onboard receiver was used to receive these signals for retransmission to the processor in the ground station. This system can provide position data to an uncertainty of less than 0.5 mi (0.8 km). The GPS signal was multiplexed into the telemetry stream and updated every 8 seconds.

All the telemetry data was sent to the ground in the form of pulse code modulation. A UHF L-band transmitter in the CIP was used to generate the RF

carrier. The L-band carrier was modulated by the pulse code and sent to the receiving station at Palestine.

An aircraft-type transponder was flown so that Air Traffic Control (ATC) could read the balloon's location on their radar systems during the descent portion of the flight. ATC was helpful in relaying to the recovery aircraft the exact position of the bottom payload during its descent on the parachute.

The purpose of the PCM command system is to send commands to the balloon - e.g., to turn the tracker on or off, terminate the flight, release ballast, etc. It was designed to reject false commands and was highly reliable in operation. The data was encoded on a frequency-shift-keyed audio carrier. This signal was then decoded into data and timing control. Each command consisted of a double transmission of the data word. Both words must be decoded and pass a bit-by-bit comparison before a command can be executed. Commands may be sent to the balloon from either the ground station at Palestine or from the recovery airplane.

The lower payload is suspended from the balloon by an 8.5-m diameter parachute. The top end of the parachute was fastened to the bottom of the balloon, and the lower payload (which contained the CIP, the battery power supply, and the ballast) was attached to the shroud lines. Appropriate electrical cables and breakaway connectors were rigged in parallel with the mechanical connections. The whole bottom assembly was designed to break away from the balloon and fall to earth while suspended from the parachute at termination of the flight.

4. FLIGHT SEQUENCE

4.1 PRELAUNCH PREPARATIONS AND LAUNCH

The balloon launch pad at the NSBF is a large circular area, 2,000 ft (600 m) in diameter. In the center of this large circle is another circular area, solidly paved, measuring 1,000 ft (300 m) in diameter. This circular launch pad allows layout of the balloon in precise alignment with the surface wind. Grass is planted in the area between the 2 circles, and a paved road surrounds the larger circle. Paved radials extend from the perimeter road toward the launch pad.

When all prelaunch preparations had been completed and the staff meteorologist had predicted favorable weather and winds at Palestine and for some 300 mi (480 km) downrange, the equipment was taken to the launch site. (Launches from Palestine are only authorized when the predicted termination point is at least 200 mi west of Palestine.)

At the launch pad, the main balloon, protected by a plastic sheath, was laid out full-length on the circular paved area. It was aligned with the direction of the wind and positioned so that the top of the balloon was on the upwind side. The top end of the balloon was passed under, then around a large, smooth, horizontal spool mounted on the front end of the launch vehicle. One end of this launching spool was hinged to the launch vehicle. The other end of the spool had a latch that could be released by a trigger mechanism. After the balloon was passed over the spool, the spool was pushed back to engage the latch so that the spool trapped the balloon. The top 10 m or so of the balloon was pulled forward from the spool, allowing the top payload to rest on the ground. It is this top 10 m of balloon that later received the helium gas during inflation. After the launching spool was latched, final preparations of the top payload began. The tow balloon was attached to the hoop with nylon lines, the clock was wound, the camera was energized, and a final checkout of the tracker and data encoder was performed.

The launch sequence began by inflating the tow balloon with helium to the point where it just lifted the top payload assembly. The main balloon was then inflated by passing a predetermined volume of helium through 2 long fill-tubes and into the balloon. The helium formed a bubble in the part of the balloon above the launching spool. Figure 6 shows the configuration of the flight train at this stage of preparation. The balloon was launched by triggering the latch on the launching spool. When the latch was released, a stout spring caused the free end of the spool to fly forward, rotating about the hinge, which released the balloon. As the balloon rose, the launch vehicle at the lower end of the balloon began to move forward (downwind). After the driver of the launch vehicle had positioned the vehicle directly below the balloon and had his vehicle going along at the same speed as the balloon, he released the latch on the pin and the lower payload was released. Figure 7 shows the balloon system and the launch vehicle a few seconds after release of the launching spool just as the downwind launch vehicle began to move. As soon as the main balloon quit oscillating, a signal was sent from the launch pad that triggered the explosive charges on the ropes connected to the tow balloon. This released the tow balloon, and the launch sequence was complete.

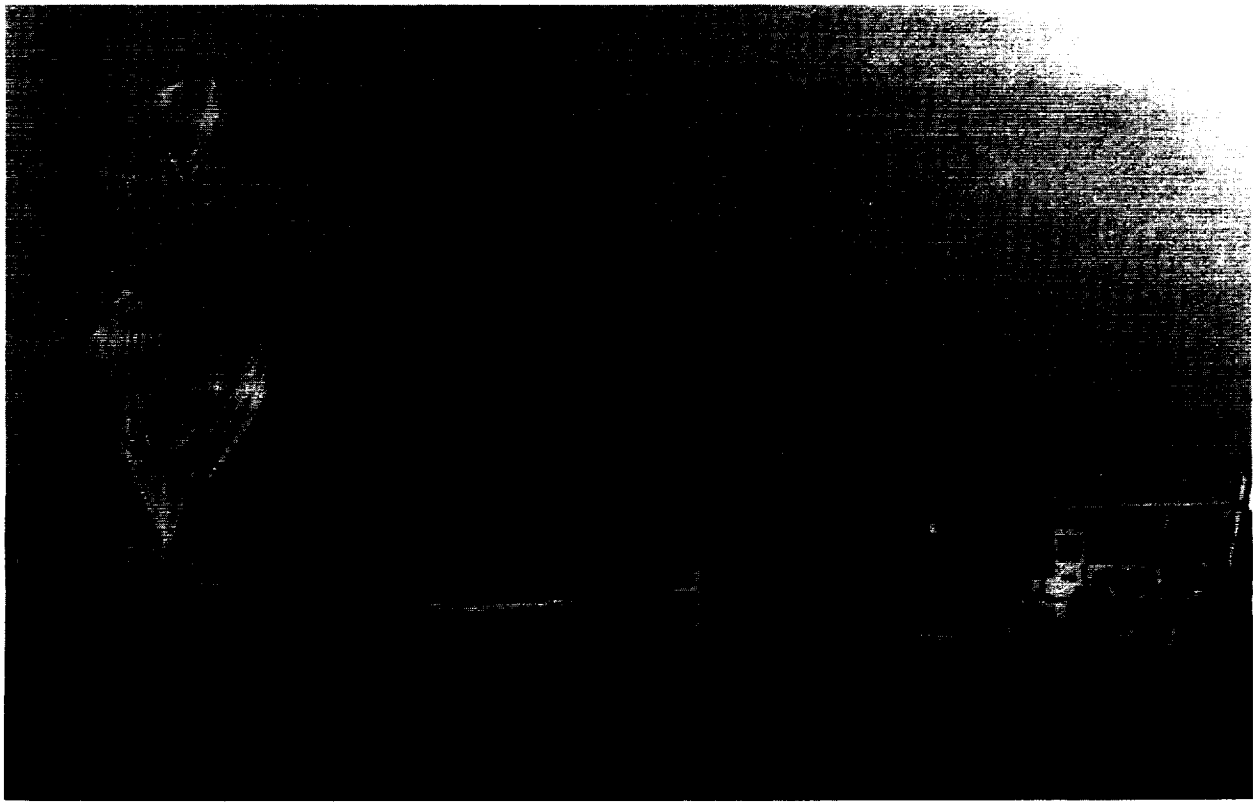

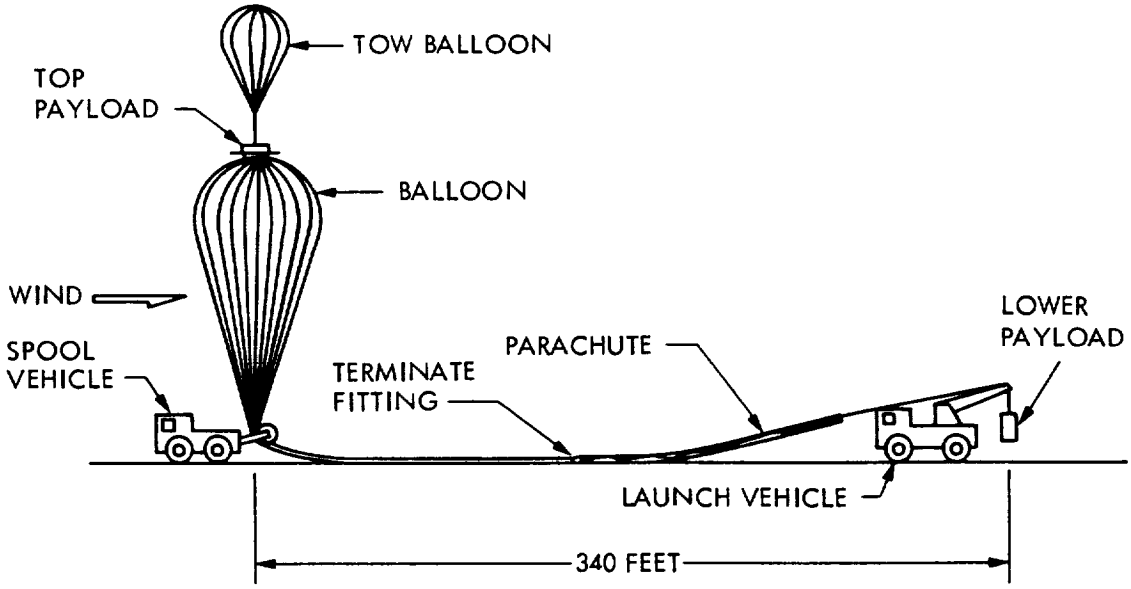

Figure 6. Flight Train Configuration

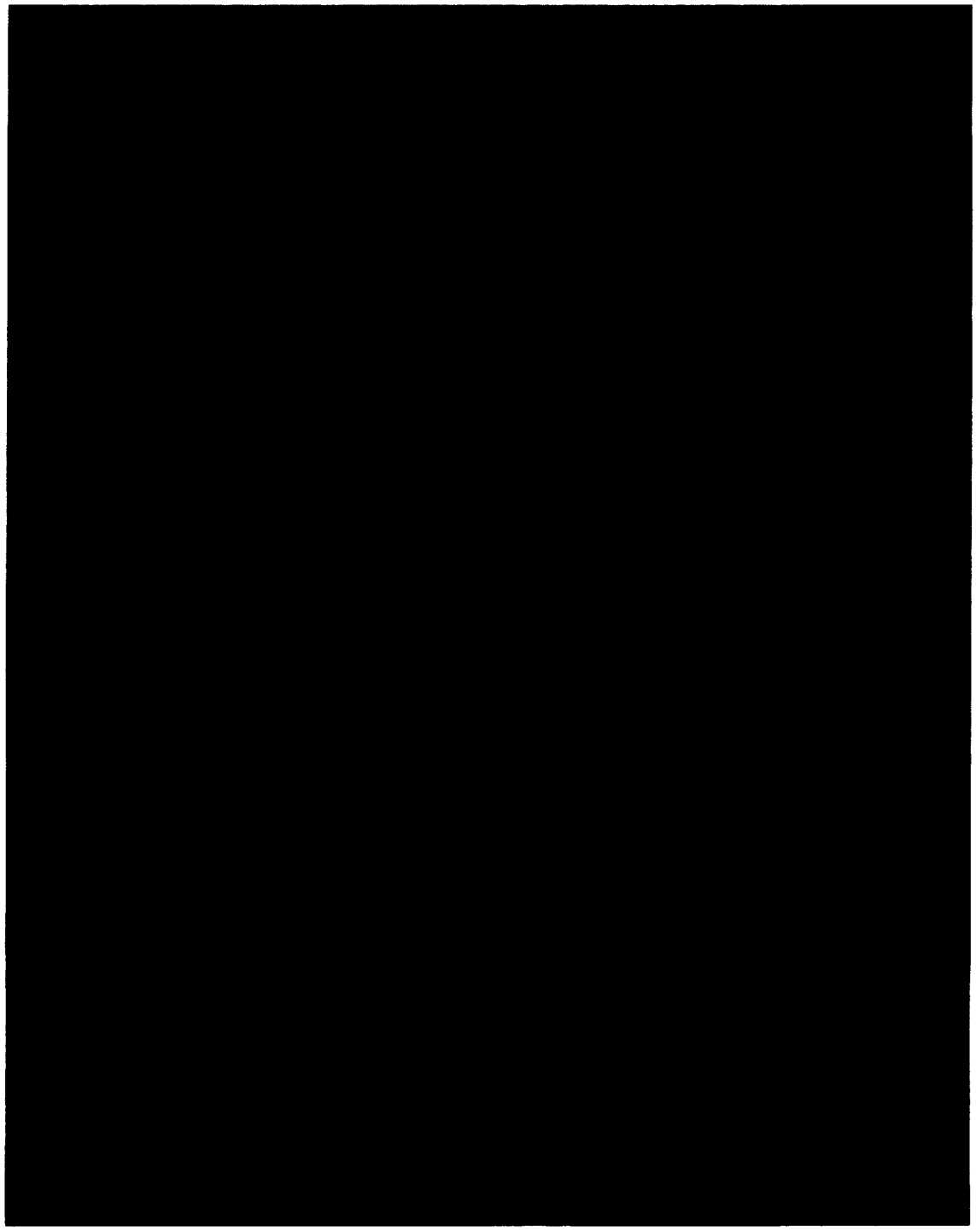

Figure 7. Balloon Launch

4.2 FLIGHT

The balloon ascended at a rate of ≈900 ft/min (4.6 m/s) and reached float altitude after ≈2 hours. During the ascent, the flight controller at Palestine maintained a constant contact with ATC. Data from the onboard navigational system was continuously given to ATC so that air traffic in the area could be vectored around the balloon.

After the balloon had been launched, solar cell voltages interspersed with reference calibration voltages and RTD voltages were fed into the telemetry system. These voltages were converted to PCM and were transmitted to the NSBF ground station along with the position, altitude, and other information from the CIP. At the ground station, the signals were decoded, recorded, and displayed in real time for monitoring of the flight.

The first balloon was launched on June 30, 1996 at 13:48 UT (8:48 local time) and reached float altitude at 17:04 UT. This was an unusually slow ascent for our payload. The tracker was turned on and achieved lock at 15:34 UT. It continued tracking and sending data until 20:46 UT.

The second balloon was launched on Aug. 8, 1996 at 12:41 UT (7:41 local time) and reached float altitude at 15:02 UT. The tracker was turned on and achieved lock at 15:38 UT. It continued to track and send data until it was commanded off and the flight was terminated at 18:52 UT. Solar noon occurred at ≈18:30 UT for each of the two flights.

4.3 FLIGHT TERMINATION

Shortly after launch, a ground recovery crew began driving toward the expected termination area in a special recovery truck. Approximately 2 hours after the balloon reached float altitude, the recovery airplane took off from Palestine with an experimenter and an observer aboard. This airplane was equipped with a telemetry receiver and computer controlled system that allowed the crew to monitor the location of the balloon and the status of its systems. Radio equipment aboard the airplane allowed communication with the balloon base and with the ground recovery crew. The airplane also had a full command system so that it could send commands to the balloon.

During the summer months, the winds at altitudes above 80,000 ft (24 km) blow from east to west at speeds of about 50 knots (25 m/s), so the airplane had to fly about 200 mi (330 km) west of Palestine to be in position for recovery. The pilot could fly directly toward the balloon at any time by flying toward the telemetered location of the balloon. This position information was generated by the GPS system on the balloon, telemetered to the Balloon Base at Palestine, and relayed from there to the airplane. The observer in the recovery airplane shared the responsibility for termination of the flight with the launch director in the NSBF control tower at Palestine. Before leaving Palestine, the recovery personnel had received a set of descent vectors from the meteorologists. The descent vectors are estimates of the trajectories that the payloads should follow as they descend by parachute. Upon receiving word that the experimenter had sufficient data, the pilot flew under the balloon to double check the accuracy of the GPS data. Using the descent vectors, he then plotted where the payloads should come down. He also established contact with ATC. When ATC advised that the descending payloads would not endanger air traffic, and when the descent vector plots showed that the payloads would not come down in an inhabited area, the observer aboard the airplane sent the commands to the balloon that terminated the flight.

The termination sequence began with a command to the balloon that disconnected power from the tracker and data encoder. Next, a command was sent that cut the cables holding the top payload onto the top of the balloon and opened the poppet valves, which began to release helium. The next command cut the electrical cable running from the bottom payload to the top payload. The fourth command released the bottom parachute from the balloon, which allowed the bottom payload to fall away and caused the balloon to become top-heavy. As the bottom payload fell, a rip line, connected from the parachute to the body of the balloon, ripped open the side of the balloon. The balloon collapsed, the top payload fell off the balloon, its parachute opened, and all 3 objects began their descent.

Typical descent time for the top payload is 40 minutes. The descent time for the bottom payload is ≈60 minutes. While the payloads are descending, the pilot monitored the position of the bottom payload by visual reference. When they had reached the ground, both payloads and the collapsed balloon had to be found. Since the bottom payload was observed at impact, locating it was not a problem, but a brief search pattern had to be flown in order to locate the balloon and the top payload. The locator beacon aided immensely in this search. This year the descent at the end of the first flight was normal. No solar cells were damaged, although the azimuth drive motor was broken. After the second flight, the payload descended through the middle of a thunderstorm, and the

panel assembly was separated from the tracker. Some cell damage occurred. During each flight, the precise locations of all 3 items were established by observation from the chase plane. The ground recovery crew was directed to each impact site by the pilot as he circled the area in the airplane.

This year the touchdown site for the first flight was near the town of Sterling City, Texas (southeast of Big Spring) ≈330 mi (530 km) from Palestine. The total flight duration from launch until the terminate command was sent was ≈7.2 hours. The second flight, which lasted ≈6.3 hours, terminated near the town of Garden City, Texas (south of Big Spring) ≈340 mi (550 km) from Palestine.

5. DATA ANALYSIS

The computer analysis was performed at JPL using a TBASIC (registered trademark of the TransEra Corp.) program written for a PC. The program read the raw data from the files produced by the LabVIEW program during the flight, then corrected the fixed-load cell data for temperature and Sun-Earth distance according to the formula:

$$V_{28,1} = V_{T,R}(R^2) - A(T - 28)$$

where

- $V_{T,R}$ = measured module output voltage at temperature T and distance R, where
- R = Sun-Earth distance in astronomical units (AU). (see reference 2)
- A = module output temperature coefficient.
- T = module temperature in degrees C.

A similar correction is made to the cells producing I-V curves. The correction shown above is made for all measured cell current values. A separate correction, utilizing a temperature coefficient appropriate for V_{oc}, is applied to the cell voltages, but the factor for Sun-Earth distance is not used. This correction is made for all measured cell voltage values.

The remainder of this section describes the details of performing the above corrections and computing calibration values for the cells.

5.1 DATA STREAM DESCRIPTION

The data is sent from the computer on the balloon to the ground telemetry station in groups called frames. Each frame consists of 26 lines of data, and each line contains 43 words of data. The first line of data contains the frame synch word, a line count word, a frame count word, time of day, temperature data, calibration voltages, power supply voltages, the on-Sun indicator reading, and a checksum word. The next 25 lines begin with a line synch word and a line count word. In line 2, this is followed by 30 data words corresponding to the outputs of the fixed-load cells (channels 21 through 50). Words 33 through 42 contain fill data (7's), and word 43 is a checksum. The fixed-load cell readings are repeated four more times and sent in lines 3 through 6 using the same format as used in line 2. Line 7 begins with the line synch word and a line count word. Words 3 and 4 contain the voltage and current readings resulting from the first load resistor applied to cell 1. The next 38 words contain the voltage and current readings for the remaining 19 loads applied to cell 1. Word 43 is again a checksum. Lines 7 through 26 contain data for the 19 I-V cells and the calibration channel in this same format. The LabVIEW program receives the data in this format and, after producing a real-time display on the computer screen, stores the data on files as it was received.

5.2 FIXED-LOAD CELLS

The computer analysis program performed its analysis in 2 steps. In the first step the cells with fixed loads are read from the files created by the LabVIEW program during the flight. The program begins by looking for the frame synch word marking the beginning of a frame. Once this word was found, the on-Sun indicator reading was decoded. If this reading was greater than the minimum allowable value (OSIMIN), analysis proceeded by applying the temperature and Earth-Sun distance corrections to the data for each of the 30 fixed-load cells. Appropriate data for each cell (sums, sums of squares, and number of readings) was accumulated for computing averages and standard deviations after all the data was read.

The temperature for each cell was computed by weighing the values of the six RTDs (T1 - T6) on the panel. That is, if cell x was located physically on the panel midway between RTDs T1 and T2, and if T1 and T2 were both mounted under the same cell types as cell x, then the temperature for cell x would be taken to be an equally weighted average of T1 and T2. But if T1 was under a different cell type than that of cell x, then the temperature of cell x might more accurately be computed by applying a higher weighting factor to T2 than to T1. A certain amount of judgement is required of the analyst in choosing the weighting factors involved in the temperature readings. This is of some importance, since

the RTDs showed that there was a temperature gradient over the panel that became stronger as the flight progressed.

The analysis of the first 1996 flight data for the fixed-load cells resulted in 1,275 readings for each cell. Data points were accepted after the balloon first reached 115,000 ft and ended as the balloon descended through 115,000 ft. During the second 1996 flight, data points were accepted after the tracker was turned on at an altitude of 118,000 ft and prior to descent through 115,000 ft. On the second flight, 845 acceptable readings were recorded for each cell. Averages and standard deviations were computed for each cell. These numbers are reported in Tables 1 and 2.

5.3 I-V CHARACTERISTIC MEASUREMENTS

The second step in the computer analysis was to extract the data from the I-V cells. In this procedure, the frame synch word was found, then the on-Sun indicator reading and the cell temperatures, just as in the procedure for the cells with fixed loads. If the on-Sun indicator reading was at or above the OSIMIN threshold level and the Sun-angle-sensor readings were below the pointing error limits, the current-voltage pairs for each cell were read. The currents were corrected for Earth-Sun distance and for cell temperature, as described for the fixed-load cells, except that this correction was applied to every current reading using the measured temperature coefficient for I_{sc}. A correction was also made to all the voltage readings using a V_{oc} temperature coefficient appropriate for each cell, but no Earth-Sun correction was made for the voltage values. The application of the current and voltage corrections is equivalent to a translation in the current and voltage axes. The data for each cell was recorded on a diskette in spreadsheet-compatible format and sent to the vendor of that cell.

5.4 CALIBRATION RESULTS

Tables 1 and 2 report the calibration values of all the fixed-load cells calibrated on the 1996 balloon flights corrected to 28°C and to 1 AU (1.496×10^8 km). The tables also report the standard deviation of the measurements, the preflight and postflight readings of each module in the X25 simulator, and a comparison of the preflight and postflight simulator readings. The simulator intensity was set with a silicon standard cell. No attempt was made to match the standard cell with each module, since the purpose of the preflight vs postflight measurements is to make sure no damage occurred to the cells as a result of the flight. The tables also report the temperature coefficients that were measured for each module in our laboratory.

5.5 DATA REPEATABILITY

Several standard modules have been flown repeatedly over the 33-year period of calibration flights. Module BFS-17A, which had flown on 41 flights, was damaged in 1990 and is no longer available. In its history of 41 flights, the BFS-17A calibration values averaged 60.180, with a standard deviation of 0.278 (0.46%). In addition to giving a measure of the consistency of the year-to-year measurements, BFS-17A also provided insight into the quality of the solar irradiance falling on the solar panel, with regard to uniformity, shadowing, or reflections. This cell had been mounted in various locations on the panel over the years. Nevertheless, its readings were always consistent, which verified that there are no uniformity, shadowing, or reflection problems with the geometry of this system.

We have identified a group of solar cells that will be used as replacements for the function served by BFS-17A. Some cells from this group will be flown every year so that we can continue our year-to-year continuity checks. Eight cells were flown from this group on the 1996 flights. Data from these eight cells is presented in Table 3. Cell 73-182 was flown on both 1996 flights. Its calibration values, 67.65 and 68.26, compared well with the average of 67.95 established over 15 flights. Four other Si cells and one GaAs cell also measured very close to the overall averages for several flights. The measurements of two GaAs/Ge cells show an apparent degradation over time. Aside from these two GaAs cells, the measurements indicate that the calibration values, using the new data acquisition system, are consistent with measurements from previous years.

5.6 I-V MEASUREMENTS

Figures 8 through 20 are the I-V curves of 13 cells that were measured on the two balloon flights. Some of the I-V data is omitted by request of the sponsors due to the proprietary nature of the cells flown. Of the curves shown, only two were of conventional Si cells (Figures 8 and 9); the rest are curves produced by dual junction cells. In some of the figures, only one curve for a particular cell is plotted. In other figures, three curves are plotted. When only one curve is shown, all the curves were virtually identical. When three curves are shown, there is a large variation in the curves, usually in the current. The three curves represent the maximum, the minimum, and the average values for cell current and maximum power. Note that several of the curves do not

give a true measure of short circuit current because the curves do not go through 0 volts. This is because the I-V curves are generated by a succession of resistive loads. The resistive load actually consists of a series string of resistances, including the current-measuring resistor (0.1 ohm), the leads from the DAQ to the cells and the load resistor(s) themselves. Even though the load resistance introduced by the program is 0 ohms, the remaining resistances in the string are sufficient to load the cell at a voltage considerably greater than 0 volts. This is particularly true for cells with large area that produce large currents.

The curves are derived from the digital telemetry data recorded during each flight. Data from the Sun angle sensor was used to select only those curves taken while the tracker was pointed at the Sun to within 2° in azimuth and 1° in elevation. Curves for the concentrator module were rejected unless the pointing accuracy was better than 2° in azimuth and 0.5° in elevation. This was because of the extreme sensitivity of this particular concentrator module to pointing errors in elevation.

Table 4 displays some statistical data about the curves depicted in the figures. For each cell, the table gives the mean, the standard deviation, the minimum measured value and the maximum measured value for 6 of the important cell parameters. These statistics apply only to the curves that fell within the pointing accuracy criteria described above.

6. CONCLUSIONS

The 1996 balloon flights were both successful. Eight cells from previous flights were reflown this year. With the exception of two GaAs/Ge cells, the 1996 measurements compared well with previous years' measurements. We believe that the agreement is very satisfactory and that the calibration values obtained from the 1996 flights can be used with a high degree of confidence.

7. REFERENCES

1. B. E. Anspaugh, R. G. Downing, and L. B. Sidwell, *Solar Cell Calibration Facility Validation of Balloon Flight Data: A Comparison of Shuttle and Balloon Flight Results*, JPL Publication 85-78, Jet Propulsion Laboratory, California Institute of Technology, Pasadena, California, October 15, 1985.

2. *The Astronomical Almanac for the Year 1996*, U.S. Nautical Almanac Office, U.S. Naval Observatory, Superintendent of Documents, U.S. Government Printing Office, Washington, DC 20402, pages C10 and C12.

Table 1. 1996-1 Balloon Flight 6/30/96 120,000 ft, RV = 1.0166707, Flight No. 1548P

MODULE CALIBRATION DATA				COMPARISON SOLAR SIMULATOR & FLIGHT			GENERAL INFORMATION	
Module Number	Org.	Temp Intensity Adjusted Average	Std Dev	AMO, Solar Sim. 1 AU 28 Deg C. Pre-Flt	Post-Flt	Post-Flt. vs. Pre-Flt. (Percent)	Temp. Coeff. (mV/C)	Comments
94-101	Hughes	78.65	0.2066	99.99	78.30	-21.69	0.07050	GaAs
96-140	Hughes	84.70	0.3053	85.38	86.39	1.18	0.09990	Bottom Cell
96-146	Hughes	77.98	0.0572	74.61	75.27	0.88	0.04730	Top Cell
96-148	Hughes	90.14	0.1784	85.66	86.42	0.89	0.05220	Top Cell, Irr.
96-151	Hughes	79.84	0.0662	78.56	79.22	0.84	0.08440	GaAs MBRR M Cvr.
96-152	Hughes	84.89	0.2468	84.88	86.23	1.59	0.14000	Bottom Cell, Irr.
96-155	Hughes	78.18	0.1159	77.09	77.78	0.90	0.06480	GaAs Irr.
73-182	JPL	67.65	0.0873	68.74	68.49	-0.36	0.04850	Heliotek Si
86-023	JPL	58.51	0.0877	57.95	58.00	0.09	0.04460	ASEC GaAs Mantech
86-026	JPL	76.06	0.0485	76.40	76.50	0.13	0.03310	ASEC K4 3/4 10 Ohm, 8 mil
95-001	JPL	77.20	0.1634	77.43	76.41	-1.32	0.04980	ASEC GaAs/Ge T3
95-002	JPL	79.71	0.2271	79.25	99.99	26.17	0.05620	ASEC GaAs/Ge T2
95-003	JPL	76.69	0.0472	76.52	76.63	0.14	0.04360	ASEC Si 2 Ohm 8 mil T4
96-005	JPL	78.52	0.3088	74.82	74.73	-0.12	0.04280	SPL Top Cell T5
96-186	SPL	88.75	0.3293	89.31	89.57	0.29	0.10190	Bottom Cell
96-190	SPL	85.62	0.2154	82.43	82.23	-0.24	0.05540	Top Cell, Irr.
96-192	SPL	79.73	0.2320	80.39	80.42	0.04	0.12540	Bottom Cell, Irr.
96-101	SS/Lor	76.45	0.0473	75.86	75.54	-0.42	0.12420	Si BFS Irradiated
95-192	TRW	77.67	0.0590	77.33	77.84	0.66	0.04780	ASE Si
96-161	TRW	80.03	0.0582	79.69	80.26	0.72	0.05850	Sharp Si Hi Eff.
96-162	TRW	79.51	0.1618	79.13	79.89	0.96	0.05940	Sharp Si Hi Eff.
96-163	TRW	88.27	0.1873	87.14	87.61	0.54	0.05200	ASE Si Hi Eff.
96-165	TRW	88.25	0.0622	87.02	87.47	0.52	0.05010	ASE Si Hi Eff.

Table 2. 1996-2 Balloon Flight 8/8/96 120,000 ft, RV = 1.0138639, Flight No. 1550P

MODULE CALIBRATION DATA				COMPARISON SOLAR SIMULATOR & FLIGHT			GENERAL INFORMATION	
Module Number	Org.	Temp Intensity Adjusted Average	Std Dev	AMO, Solar Sim. 1 AU 28 Deg C. Pre-Flt	Post-Flt	Post-Flt. vs. Pre-Flt. (Percent)	Temp. Coeff. (mV/C)	Comments
96-108	EEV	84.13	0.0839	83.48	83.25	-0.28	0.05700	GaAs
95-101	Hughes	72.31	0.1351	72.21	72.67	0.64	0.07200	GaAs/Ge 4 x 6 Refly
96-157	Hughes	82.61	0.0409	79.84	79.33	-0.64	0.05010	GaAs Dual Jcn.
73-182	JPL	68.26	0.3093	68.74	68.49	-0.36	0.04850	HEK Si
80-003	JPL	78.40	0.0688	78.26	78.20	-0.08	0.04390	SPL K4 3/4
81-004	JPL	77.10	0.2398	76.98	77.25	0.35	0.04840	K 4 3/4 BSR
STS021	JPL	72.85	0.0579	73.41	73.50	0.12	0.05400	Hi Blue
92-005	JPL	57.23	0.2303	57.57	56.48	-1.89	0.04090	GaAs/Ge
95-002	JPL	79.53	0.3671	79.25	78.29	-1.21	0.05620	ASEC GaAs/Ge T5
95-003	JPL	76.67	0.0514	76.52	76.63	0.14	0.04360	ASEC 2 ohm-cm Si
96-001	JPL	77.26	0.2613	77.48	77.63	0.19	0.09050	ASEC Dual Jcn Bott Limit
96-002	JPL	76.16	0.2650	76.31	76.38	0.09	0.09070	ASEC Dual Jcn Bott Limit
96-005	JPL	78.28	0.0304	74.82	74.73	-0.12	0.04280	SPL Top Jcn. T4
96-006	JPL	77.53	0.4122	87.88	77.83	-11.44	0.08000	SPL Bottom Jcn.
96-007	JPL	77.88	0.1730	88.83	78.48	-11.65	0.08410	SPL Bottom Jcn.
96-180	SPL	83.22	0.1669	82.24	81.85	-0.47	0.06770	GaAs/Ge
96-184	SPL	82.87	0.0767	79.85	79.57	-0.35	0.05140	Top Cell
96-103	SS/Lor	74.08	0.0516	74.09	73.62	-0.63	0.04000	Si BSF
92-131	TRW	32.09	0.0869	32.66	32.52	-0.43	0.04280	Amorphous Si

Table 3. Repeatability of Eight Standard Solar Cell Modules Over a 22-year Period

Flight Date	73-182 HEK	80-003 K4 3/4	81-004 K4 3/4 BSR	STS-021 Hi Blue	86-023 Mantech GaAs	86-026 K4 3/4	92-005 GaAs/Ge	95-002 GaAs/Ge
4/5/74	68.37							
6/6/75	67.88							
6/10/77	67.96							
7/20/78	68.20							
8/8/79	67.83							
7/24/80	68.00	78.69						
7/25/81	67.96		77.55					
7/21/82	68.03		77.52					
7/12/83	68.03							
7/19/84	67.62							
8/84 Shuttle				73.60				
7/12/85				72.85				
7/15/86					58.46	76.25		
8/23/87					59.47			
8/7/88			77.49		58.26			
8/9/89					58.30			
9/6/90			77.43		58.89			
8/1/91				73.08	59.12		62.31	
8/1/92		78.30			58.68	76.29	60.92	
7/29/93	67.71		77.24			76.03		
8/6/94	67.77	78.51			58.91	75.82		
8/31/95	67.95				58.69			81.53
6/30/96	67.65				58.51	76.06		79.71
8/8/96	68.26	78.40	77.10	72.85			57.23	79.53
No. of Meas.	15	4	6	4	10	5	3	3
Average	67.95	78.48	77.39	73.10	58.73	76.09	60.15	80.26
Std. Deviation	0.217	0.167	0.179	0.354	0.378	0.189	2.625	1.106
Max. Value	68.37	78.69	77.55	73.60	59.470	76.29	62.31	81.53
Min. Value	67.62	78.30	77.10	72.85	58.260	75.82	57.23	79.53
Max.	0.422	0.215	0.288	0.505	0.741	0.270	2.923	1.273

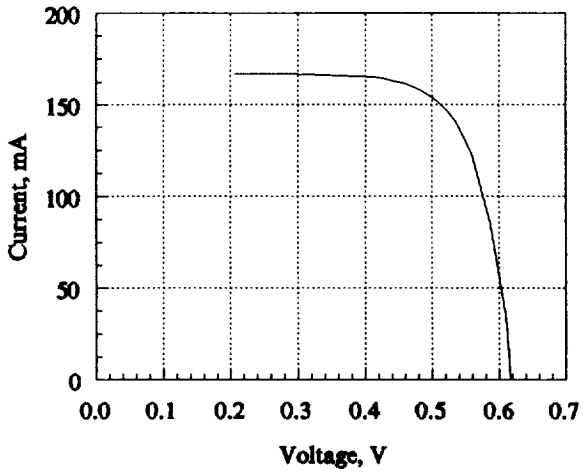

Figure 8. 95-004, Tecstar Si Cell, 10 Ohm-cm, 8 mils Thick, Flown on 1996 Flight 1

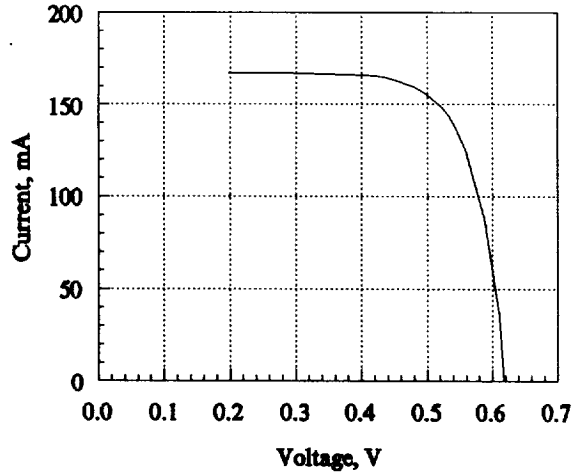

Figure 9. 95-004, Tecstar Si Cell, 10 Ohm-cm, 8 mils Thick, Flown on 1996 Flight 2

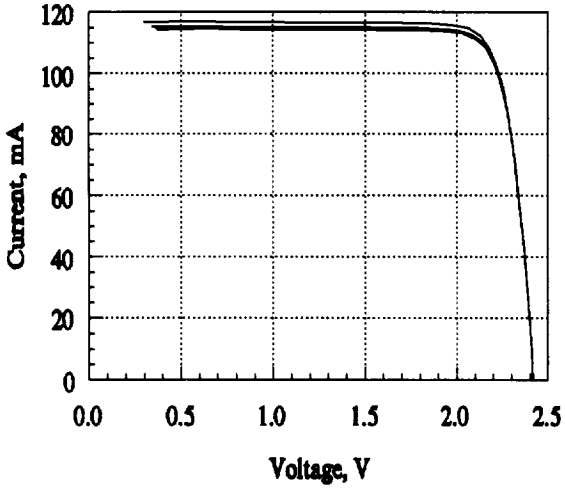

Figure 10. 96-004, Tecstar Dual Junction Cell, Bottom Limiting

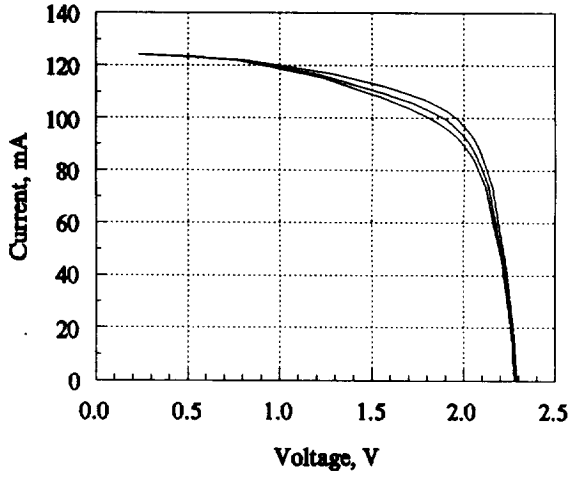

Figure 11. 96-003, Tecstar Dual Junction Cell, Top Limiting

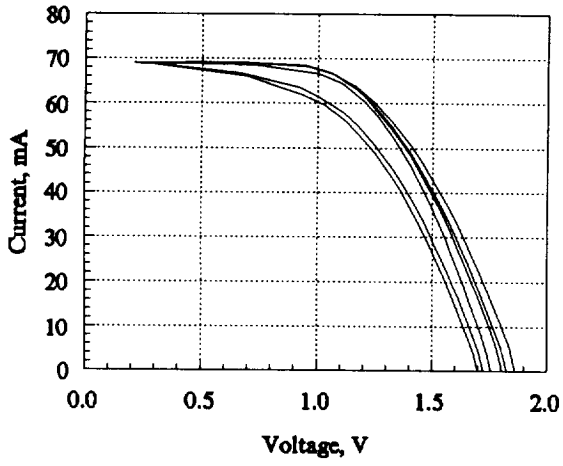

Figure 12. 96-138, Tecstar Dual Junction Cell, Concentrator Design

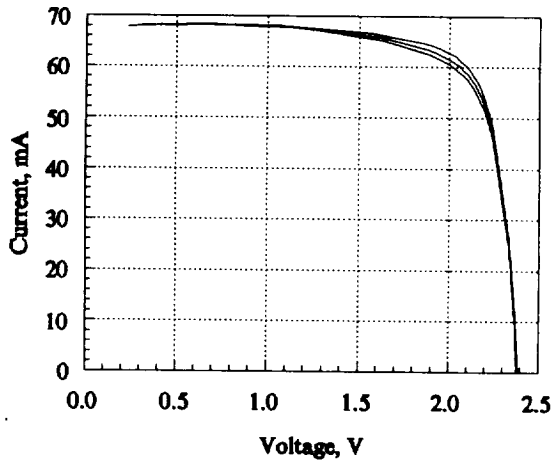

Figure 13. 96-346, Tecstar Dual Junction Cell, Concentrator Design

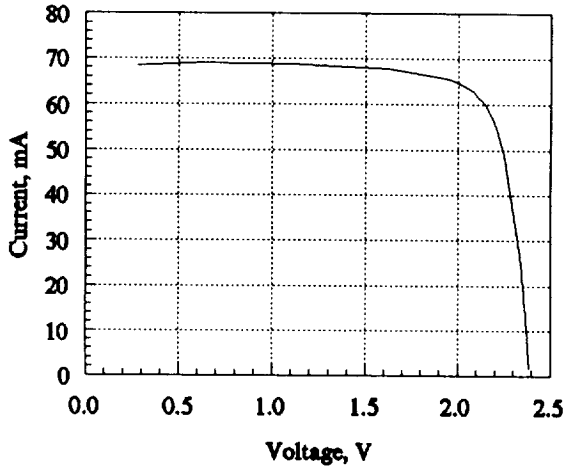

Figure 14. 96-308, Tecstar Dual Junction Cell, Concentrator Design

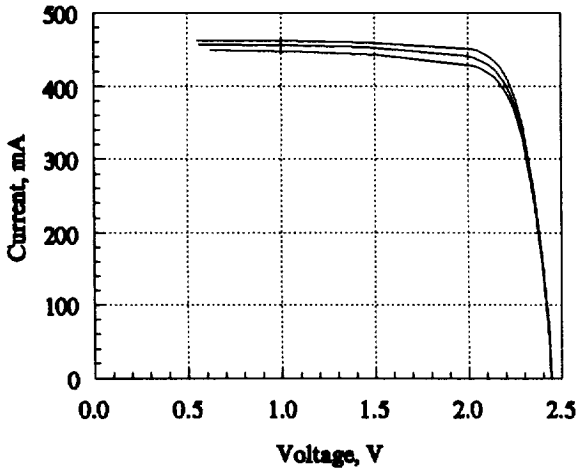

Figure 15. 96-359, Tecstar Dual Junction Cell in Linear Concentrator Module

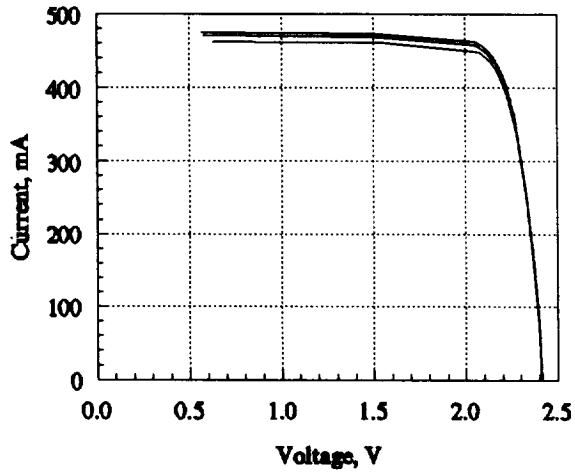

Figure 16. 96-304, Tecstar Dual Junction Cell in Linear Concentrator Module

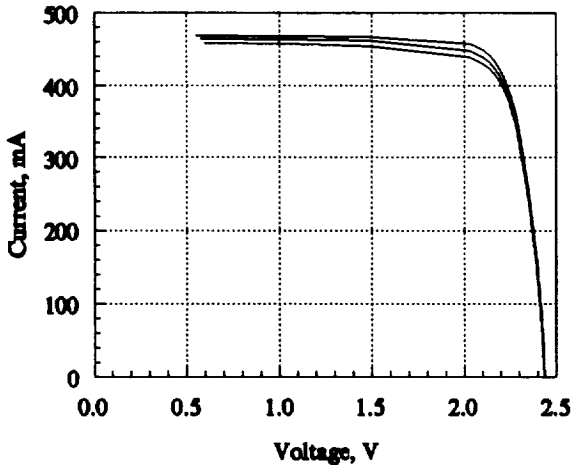

Figure 17. 96-352, Tecstar Dual Junction Cell in Linear Concentrator Module

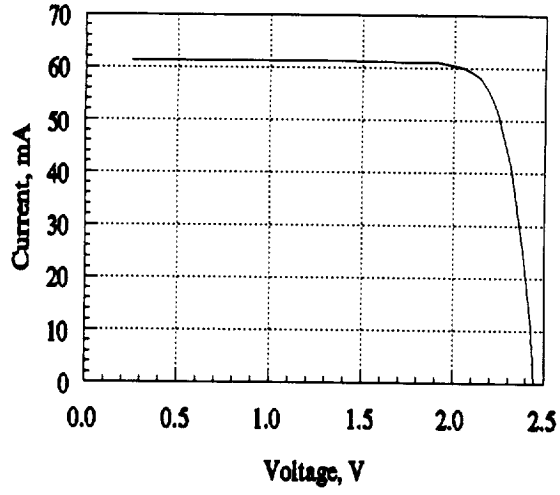

Figure 18. 96-202, Tecstar Dual Junction Cell

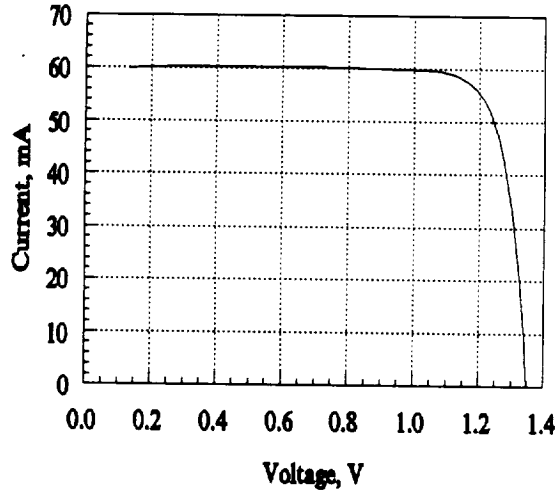

Figure 19. 96-201, Spectrolab Top Cell of Dual Junction Cell Design

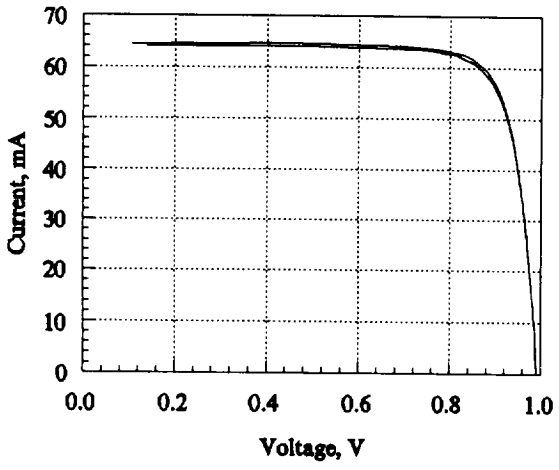

Figure 20. 96-204, Spectrolab Bottom Cell of Dual Junction Cell Design

Table 4. Statistical Data for the Cells with I-V Measurements

95-004 Flight 1						
	Isc	Voc	Imp	Vmp	Pmax	FF
Average	166.83	617.08	151.49	507.81	76.92	0.747
Std. Dev.	0.167	1.331	1.096	3.896	0.133	0.003
Min.	166.50	614.00	150.00	496.80	76.70	0.742
Max.	167.40	619.50	154.50	513.90	77.30	0.755
95-004 Flight 2						
	Isc	Voc	Imp	Vmp	Pmax	FF
Average	167.49	617.90	153.40	505.90	77.64	0.750
Std. Dev.	0.111	0.700	1.020	3.400	0.071	0.002
Min.	167.26	616.60	150.88	501.70	77.50	0.747
Max.	167.71	619.80	154.77	514.80	77.81	0.753
96-003 Flight 1						
	Isc	Voc	Imp	Vmp	Pmax	FF
Average	124.15	2283.10	98.88	1907.70	188.62	0.666
Std. Dev.	0.099	4.600	1.600	24.600	3.743	0.012
Min.	123.91	2274.10	95.80	1874.40	182.53	0.646
Max.	124.59	2290.70	102.53	1959.20	195.88	0.689
96-004 Flight 1						
	Isc	Voc	Imp	Vmp	Pmax	FF
Average	115.27	2417.58	110.57	2133.82	235.93	0.847
Std. Dev.	0.411	1.975	1.235	17.416	1.017	0.002
Min.	114.34	2410.40	108.62	209.48	233.81	0.843
Max.	116.74	2421.00	113.09	215.67	239.21	0.849
96-138 Flight 1						
	Isc	Voc	Imp	Vmp	Pmax	FF
Average	68.88	1763.50	58.65	1166.90	68.47	0.563
Std. Dev.	0.069	44.500	2.597	35.900	4.272	0.022
Min.	68.63	1703.40	54.49	1107.10	62.68	0.534
Max.	69.19	1864.50	63.29	1243.70	74.96	0.597
96-201 Flight 1						
	Isc	Voc	Imp	Vmp	Pmax	FF
Average	59.90	1346.87	57.42	1167.89	67.06	0.831
Std. Dev.	0.134	1.240	0.458	10.268	0.106	0.003
Min.	59.62	1344.90	56.41	1151.90	66.88	0.826
Max.	60.11	1349.80	58.08	1189.40	67.33	0.838
96-202 Flight 2						
	Isc	Voc	Imp	Vmp	Pmax	FF
Average	61.25	2443.80	58.80	2117.50	124.51	0.832
Std. Dev.	0.066	1.600	0.429	15.300	0.181	0.001
Min.	61.17	2441.10	58.30	2081.30	123.99	0.829
Max.	61.42	2446.30	59.70	2137.40	124.99	0.835

Table 4. Statistical Data for the Cells with I-V Measurements (Cont'd)

96-204 Flight 1						
	Isc	Voc	Imp	Vmp	Pmax	FF
Average	64.15	990.57	60.49	857.79	51.88	0.816
Std. Dev.	0.137	0.760	0.390	4.788	0.184	0.002
Min.	63.89	989.20	59.41	850.70	51.54	0.811
Max.	64.46	992.00	61.56	870.70	52.38	0.822
96-304 Flight 2						
	Isc	Voc	Imp	Vmp	Pmax	FF
Average	468.97	2417.00	447.55	2105.70	942.38	0.832
Std. Dev.	3.482	0.700	3.225	13.400	6.719	0.001
Min.	461.21	2415.50	440.22	2083.90	928.94	0.830
Max.	474.81	2418.70	454.52	2124.90	954.27	0.835
96-308 Flight 2						
	Isc	Voc	Imp	Vmp	Pmax	FF
Average	68.56	2383.20	62.79	2074.60	130.26	0.797
Std. Dev.	0.143	2.600	0.480	19.100	0.400	0.002
Min.	68.18	2376.10	61.63	2029.10	129.26	0.793
Max.	68.97	2387.80	63.94	2105.80	131.09	0.802
96-346 Flight 1						
	Isc	Voc	Imp	Vmp	Pmax	FF
Average	67.88	2382.83	60.25	2053.24	123.69	0.765
Std. Dev.	0.096	7.000	0.828	20.226	1.385	0.009
Min.	67.71	2380.30	59.14	2025.80	121.05	0.747
Max.	68.07	2384.10	62.20	2092.70	126.45	0.781
96-352 Flight 2						
	Isc	Voc	Imp	Vmp	Pmax	FF
Average	464.46	2439.10	436.12	2117.90	923.62	0.815
Std. Dev.	2.577	0.800	5.622	13.400	10.983	0.005
Min.	458.20	2437.60	423.14	2103.40	903.05	0.806
Max.	468.71	2441.00	447.34	2140.30	942.88	0.825
96-359 Flight 2						
	Isc	Voc	Imp	Vmp	Pmax	FF
Average	456.17	2446.80	425.46	2127.90	905.34	0.811
Std. Dev.	3.475	0.600	6.325	6.700	14.085	0.007
Min.	448.15	2445.30	412.85	2113.10	881.53	0.803
Max.	461.68	2448.40	436.28	2139.50	931.56	0.825